

A Novel Multi-lane Detection and Tracking System

Kun Zhao*, Mirko Meuter†, Christian Nunn†, Dennis Müller†, Stefan Müller-Schneiders† and Josef Pauli*

* Intelligent Systems Group, University of Duisburg-Essen
D-47057 Duisburg, Germany
kun.zhao@stud.uni-due.de
josef.pauli@uni-due.de

† Delphi Electronics & Safety
D-42119 Wuppertal, Germany
Mirko.Meuter@delphi.com
Stefan.Mueller-Schneiders@delphi.com

Abstract—In this paper a novel spline-based multi-lane detection and tracking system is proposed. Reliable lane detection and tracking is an important component of lane departure warning systems, lane keeping support systems or lane change assistance systems. The major novelty of the proposed approach is the usage of the so-called Catmull-Rom spline in combination with the extended Kalman filter tracking. The new spline-based model enables an accurate and flexible modeling of the lane markings. At the same time the application of the extended Kalman filter contributes significantly to the system robustness and stability. There is no assumption about the parallelism or the shapes of the lane markings in our method. The number of lane markings is also not restrained, instead each lane marking is separately modeled and tracked. The system runs on a standard PC in real time (i.e. 30 fps) with WVGA image resolution (752×480). The test vehicle has been driven on the roads with challenging scenarios, like worn out lane markings, construction sites, narrow corners, exits and entries of the highways, etc., and good performance has been demonstrated. The quantitative evaluation has been performed using manually annotated video sequences.

I. INTRODUCTION

Modeling lanes or lane markings plays an important role in lane detection and tracking methods. A linear model makes the assumption that the lane is straight. In [1] a linear model is applied for lane detection at night. The linear model is feasible when the detection range of the camera system is limited, and hence the lane markings in the detection range can be approximated as straight lines. However, the simplicity of a linear model also restrains its application. In a lane departure warning system the detection range needs to be 30 meters or more in order to accurately predict the trajectory of the ego-vehicle ahead [2]. For this application a linear model is not suitable. An intuitive extension is the piecewise linear models as applied in [3] [4]. Here, several linear models are connected with specific angles to approximate a curve.

The second-order parabolic model has been commonly applied by other research groups, either in the vehicle coordinate system [2] [5] [6], or in the image coordinate system [7]. A second-order parabola fits the lane marking better than the simple linear model at curves, but it still can not model some shapes of lane markings. For example, the connection between a straight lane and a circular curve is usually constructed with a constant changing curvature,

which can only be described using a higher order curve model. There are also models that instead of the parabola use the circumference model [8] [9].

With a third-order model the linear curvature change of a lane marking can be modeled, it is normally applied as the guideline for the construction of the highways in many countries, for example in Germany [10]. Using a third-order model between a straight lane and a parabolic curve the lane curvature varies from zero linearly to a constant value. This gives the driver a more smooth steering feeling. In [11] [12] the third-order curve is used to model the horizontal curvature of the lane. Furthermore, a second-order model is also deployed in [11] to model the lane vertical curvature. One drawback of a higher order model is that it is more sensitive to detection noise, therefore a temporal filtering is necessary for robust detection.

Splines are piecewise polynomial curves. To our knowledge the spline-based lane model is first proposed by Yue Wang et al. in [13] using the Catmull-Rom spline. In [14] the spline model was further researched using the cubic B-spline. At each frame the vanishing points of separate image ROIs are first estimated, and then used for the calculation of the control points of the B-spline. The lane is modeled as a center line with lateral offsets. A fundamental assumption of both methods in [13] and [14] is the parallelism of the lane markings. In [15] the cubic spline model is used for the model fitting. The detected lane marking pixels are connected to short line segments and then fitted to several hypotheses using a cubic spline model and the RANSAC technique. The tracking method applied in [15] is a probabilistic scheme that selects a most probable lane marking from the fitting hypotheses.

The parallelism of lane markings is assumed in lots of other works i.e. [8] [13][14]. This constraint also indicates the existence of both sides of the lane markings, if a center-width model is used as in [16]. This assumption is not always valid: worn out markings are normal on the road surfaces, lane markings could be covered by other vehicles and shadows. Another constraint in these systems is that only two markings can be detected and tracked. In real applications multiple markings could be painted on road surfaces, and these markings are not always parallel. This scenario could be critical for a system that depends on

the parallelism assumption and can only detect two lane markings. If this scenario shows up, it becomes necessary to switch off the driver assistant system in order to prevent false actions or warnings.

II. SYSTEM MODULES

Our lane detection and tracking system consists of five sequentially connected modules. Figure 1 provides an overview over the system function blocks. The hardware components, like camera, yaw rate sensor or velocity sensor, provide the input data for the system. The system gives the control points of splines as output.

The line detection module uses a modified and enhanced version of the Fast Hough Transform presented by Meuter et al. [5]. The advantage of this approach is the possibility to extract lines with linear time. The detection range of the system is set to be a fixed value in the vehicle coordinate system. In a single-view camera system with the flat planar assumption this fixed detection range corresponds to a specific part of the original image. This part of image is further divided into several ROIs longitudinally, and the line detection algorithm is applied on each of them. This division is necessary for a better detection performance, because the camera projection has different scales according to the detection distance. The detections are not only tracked, but also used to recalibrate the camera online and to adjust it to the road geometries.

The classification module analyzes the image and classifies each line segment as left side or right side of a lane marking, or rejects the detection completely. The classifier uses the gradient magnitudes and directions, which can be extracted as introduced in [5].

The tracking module assigns line segments that were classified as left or right side to existing lane markings, or uses the detection to initialize a new lane marking candidate track, when certain conditions are met. In the line detection and classification modules there are no assumption about the form of the lane markings, and only short line segments which possibly belong to the lane markings are detected. So the tracking module fuses the detections for different regions into one lane marking estimation and maintains a list of several lane marking candidates over time. The temporal filtering of the tracking module provides the robustness and stability to the detected lane marking candidates. The tracking module also tries to identify parallel lane markings and improves their estimations using a fusion scheme which exploits the identical course of the lane markings.

The lane marking candidates are verified in the verification module. There are other objects on the roads which have line structures, like road poles or guard rails. These objects could possibly pass the gradient analysis in the classification module, and a false marking tracker could be initialized. The verification module is responsible to filter out false lane marking candidates and categorize the lane marking into different classes, like dashed or continuous lane marking using a temporal analysis of the input signal.

Finally, a lane marking selection module selects the relevant recognized lane markings of the lane, in which the vehi-

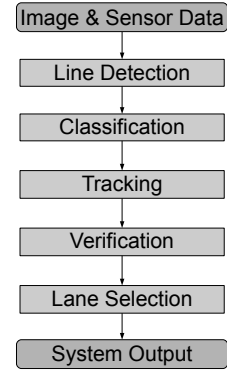


Fig. 1: Overview of our multiple lane marking detection and tracking system. The system modules are represented with rectangles.

cle is driving. This module utilizes the width, direction and parallelism information of lane markings for the selection. If the markings are overlapped, which can happen at the construction sites, this module selects the most possible lane markings. The figure of a construction site in the evaluation section provides an intuitive demonstration of the necessity of such a function module in a multi-lane detection and tracking system.

The lane marking model plays an important role in the system. The spline model does not only provide the flexibility for the modeling, but also make it possible for the multi-lane detection and tracking by removal the parallelism assumption. The splines are polynomial curves whose shapes are defined by a sequence of points, which are called control points. The Catmull-Rom spline applied in our system is an interpolation spline. Its control points lie on the spline curve, and the detection results can be easily associated with the control points in the extended Kalman filter.

III. SPLINE-BASED MODEL FOR THE TRACKING OF LANE MARKINGS

For the lane tracking module the input data is a set of line segments detected in one single frame. These line segments are classified as left or right side of a lane marking based on the gradient analysis. Using the extended Kalman filter the detection results are fused.

A. Using Catmull-Rom Splines for Lane Marking Representation

A cubic polynomial is defined as

$$p = \begin{bmatrix} \frac{1}{6}l^3 & \frac{1}{2}l^2 & l & 1 \end{bmatrix} \begin{bmatrix} a \\ b \\ c \\ d \end{bmatrix}, \quad (1)$$

where l denotes the position on one axis and the four parameters a , b , c and d specify the form of the curve. In a simple system the lane markings can be represented using this term, and by estimation of the parameters the local

course of lane markings can be modeled. In such a system, the parameters a, b, c and d are a part of the state vector \mathbf{x} and the lane representation is thus given as function

$$f(\mathbf{x}, l) = \begin{bmatrix} \frac{1}{6}l^3 & \frac{1}{2}l^2 & l & 1 \end{bmatrix} \mathbf{x} \quad (2)$$

The piecewise cubic splines are defined by a set of control points, and each the spline curves is defined as equation 1 between adjacent control points. For the i section of the splines with two control points p_i and p_{i-1} and correspondingly the slope p'_i and p'_{i-1} , the spline curve is defined in equation 3 by applying the C^0 and C^1 continuity. The spline parameters depend only on the slope and the position of the control points, so the spline parameters for section i can be obtained by solving the equation 3 [17], which is abbreviated in equation 4.

$$\begin{bmatrix} \frac{1}{6}l_i^3 & \frac{1}{2}l_i^2 & l_i & 1 \\ \frac{1}{2}l_i^2 & l_i & 1 & 0 \\ \frac{1}{6}l_{i-1}^3 & \frac{1}{2}l_{i-1}^2 & l_{i-1} & 1 \\ \frac{1}{2}l_{i-1}^2 & l_{i-1} & 1 & 0 \end{bmatrix} \begin{bmatrix} a_i \\ b_i \\ c_i \\ d_i \end{bmatrix} = \begin{bmatrix} p_i \\ p'_i \\ p_{i-1} \\ p'_{i-1} \end{bmatrix} \quad (3)$$

$$\mathbf{A}_i \mathbf{s}_i = \mathbf{b}'_i \quad (4)$$

For the Catmull-Rom splines the slope at p_i and p_{i-1} is defined using two extra adjacent control points p_{i-2} and p_{i+1} as

$$\begin{bmatrix} p_i \\ p'_i \\ p_{i-1} \\ p'_{i-1} \end{bmatrix} = \begin{bmatrix} 0 & 1 & 0 & 0 \\ \frac{1}{2} & 0 & -\frac{1}{2} & 0 \\ 0 & 0 & 1 & 0 \\ 0 & \frac{1}{2} & 0 & -\frac{1}{2} \end{bmatrix} \begin{bmatrix} p_{i+1} \\ p_i \\ p_{i-1} \\ p_{i-2} \end{bmatrix} \quad (5)$$

$$\mathbf{b}'_i = \mathbf{B} \mathbf{b}_i. \quad (6)$$

Following this definition and rearranging the equations, the spline between two control points is defined as a linear equation given by

$$f(\mathbf{b}_i, l) = \begin{bmatrix} \frac{1}{6}l^3 & \frac{1}{2}l^2 & l & 1 \end{bmatrix} \mathbf{A}_i^{-1} \mathbf{B} \mathbf{b}_i \quad (7)$$

for all l between l_i and l_{i-1} . One should note that it is possible to keep \mathbf{A}_i^{-1} constant using a proper normalization scheme, which allows to pre-calculate these matrices to save computation time. However, this technique is out of the scope of this paper. The novel idea in this paper is the estimation of the spline control point positions in an extended Kalman filter for the tracking of lane markings. Let the control point vector \mathbf{b}_i be a sub-vector of the state vector \mathbf{x} . For this case, a selection matrix \mathbf{C}_i which selects the proper elements from the state vector \mathbf{x} can be used to describe a point p on the lane marking and the state vector \mathbf{x} as

$$p = f(\mathbf{x}, l)_i = \begin{bmatrix} \frac{1}{6}l^3 & \frac{1}{2}l^2 & l & 1 \end{bmatrix} \mathbf{A}_i^{-1} \mathbf{B} \mathbf{C}_i \mathbf{x}. \quad (8)$$

The only difference to function 2 is that with different \mathbf{C} matrix equation 8 differs for different sections i . However, by using this definition and proper extrapolation schemes at the beginning and the end of the spline, to extend the representation of the lane marking to infinity, the formula above can be used to replace existing lane representation functions.

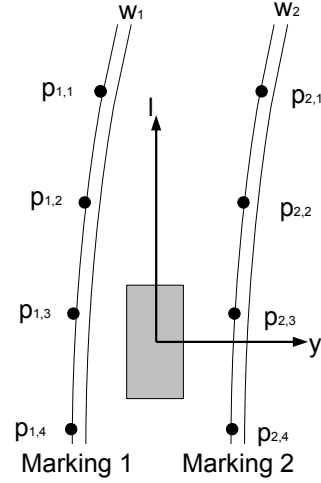


Fig. 2: An example of the representation of the splines using four control points. Axis l represents longitudinal offset in the vehicle coordinate, and y represents the lateral offset.

B. State Vector

Each state vector represents the local course of a lane marking. The state vector contains a set of control points and the width of the lane marking. The state vector \mathbf{x} , which contains the positions of the control points and the width w in the vehicle coordinate system, is defined as

$$\mathbf{x} = [p_1, p_2, \dots, p_{n-1}, p_n, w]^T, \quad (9)$$

where p_i denotes the position of control point i , w the width of the lane marking and n denotes the number of the control points used to model the lane marking. To be able to extract the width of a lane marking the line detector has to be able to extract each side of a lane marking segment separately. For the estimation an extended Kalman Filter is used. In figure 2 a lane with two lane markings is shown. Both markings are modeled using the splines. Here, each lane marking contains four control points, but of course the model can be extended to use more control points. The origin of the vehicle coordinate system lies at the gravity center of the vehicle.

C. Motion Model

In the motion model the position of each control point is stationary in the world coordinates. This simplifies the motion model to a pure ego motion compensation model of stationary points. In another words, the control points are moved in the vehicle coordinate system according to the vehicle ego movement. The stationary points in world coordinate prevents the re-sampling of the control points,

which would lead to an inconsistent model in the Catmull-Rom spline model. As motion model, a simplified model for ego motion compensation as in [5] can be used. The simplification reduces the data and computation cost, while good performance is still provided in our system, which will be demonstrated in the evaluation section.

With the vehicle moving forward all the control points flow backwards. This requires new control points to be added in front of the vehicle and old control points to be removed once they are passed and do not influence the lane marking estimation in the visible area. In such a case the remaining control points are shifted backwards in the state vector, and a new point is added in the front using a proper extrapolation scheme, the number of control points n is always kept constant.

D. Measurement model

Formula 8 can be used to formulate the measurement process in the Kalman filter for the different section. The system detects the position of the left and right lane marking borders for different distances. In the current system, a measurement formulation similar to [5] is used. The measurement \mathbf{y} is defined as a position measurement in image coordinates for a certain distance. Let the function $\mathbf{g}(\mathbf{p}_w)$ denote the projection of a point on the lane marking border given in vehicle coordinates to the image plane. The function is e.g. described in [18].

A connection between a certain distance and a point on the lane marking border can be established using the relations described in 8 to create a function

$$\mathbf{p}_w = \mathbf{f}(\mathbf{x}, l) \quad (10)$$

which allows to model the measurement process for a certain distance l_i using a nested function

$$\mathbf{y} = \mathbf{g}(\mathbf{f}(\mathbf{x}, l))|_{l=l_i} \quad (11)$$

The projection to the image plane is usually a nonlinear function, thus an extension for the Kalman filter for nonlinear systems like the extended Kalman filter has to be used here. The relationship allows to recursively estimate the position of the adjacent control points and thus the local course of the lane marking for each section. The longer a section is observed, the more accurate the control point estimates become for that section, which gives the filter a much higher stability compared spline fits based on single frame, as it was done in previous publications [14].

E. Initialization of the Tracker

Each detection result is first tested to be assigned to an existing lane marking. If this fails and certain prerequisites are satisfied, a new tracker for lane marking is initialized. The detection range of the camera system relies on the physical properties of the camera, its mounting position and angle. Because of the projection of the 3D world to the 2D image plane the detection results in the short range are considered more accurate than those lying far away. So only the detection results that lie in a specific range can be chosen

for the initialization of a new lane marking. By doing this false initialization could be strongly avoided.

The initialization procedure applies a second-order parabola to approximate the lane marking. By setting the parameter $a = 0$ the equation 1 becomes a second-order parabola:

$$y = \frac{1}{2} \cdot b \cdot x^2 + c \cdot x + d \quad (12)$$

the slope c and intercept d come from the line detection results, the curvature could be calculate approximately as $b = \frac{\varphi}{v}$. φ is the yaw rate, v is the velocity. On the parabola curve n points can be sampled at the longitudinal offsets in vector L , these points are set as the initial control points for the splines.

F. Lane Merging Detection

The possible merging of two markings can be detected by determination of the intersection of the piecewise spline curves. Furthermore, the position of the intersection can also be determined, The merged markings share partially common control points. After comparing the state vectors the common parts of the merged markings can be determined. The marking which initialized earlier is set as the master, and the other one is set as the slave. The master marking is updated by the extended Kalman filter as usual. On the contrary the slave marking is just partially updated, its common control points and corresponding covariances are directly copied from the master marking.

The concept of merging detection is simple and effective, the same idea could also be used for the lane splitting detection. The difference is that a lane splits in the far range, and under the accuracy consideration a lane marking tracker is only initialized in near detection range. Because of this the splitting detection mechanism is not implemented in our system yet.

G. Clustering of Lane Markings

In many cases there are parallel lane markings in the images. The parallelism property is not assumed in our lane marking model, which extends the application of our method. But this property can be estimated from the tracked lane markings, and used to improve the lane marking estimation. The system runs through the list of tracked lane markings and clusters those which are parallel. Afterward all lane marking estimates in a certain cluster are fused to improve the the estimates of the road lane markings. The difference vector \mathbf{d}_j between the control points encodes the course of marking j as

$$\mathbf{d}_j = [p_2 - p_1, \dots, p_n - p_1]^T \quad (13)$$

is used to detect, whether two lane markings follow a similar course and to calculate a fused road course. The difference of two \mathbf{d} vectors \mathbf{d}_i and \mathbf{d}_j can be used to detect a possible parallelism of lane markings i and j by detecting, whether the normalized distance squared of the difference vectors falls below a certain threshold [19]. If parallelism is detected in multiple frames, the lane markings are clustered together. As clustering scheme the Hierarchical

Agglomerative Clustering Algorithm is used [20]. To split clusters, a regular check is performed to determine whether the members of the cluster would be clustered together. So the same procedure can be used not only for clustering the markings together, but also for splitting of them. If two lane markings are within the same cluster, a fused \mathbf{d}_f vector can be calculated according to [19]. Afterward, an improved estimate for marking j can be generated as

$$\mathbf{x}_{f_j} = [d_{f_i} + p_1, d_{f_{i-1}} + p_1, \dots, p_1, w] \quad (14)$$

where \mathbf{d}_{f_i} denotes the entry i in the fused vector.

IV. EVALUATION

The video sequences from the evaluation database are manually labeled using the same software tool in [5]. At a fixed longitudinal distance the lateral offsets of the left side and right markings of the lane, in which the vehicle is driving, is manually marked as the ground truth.

The inner lateral offsets of the detected and tracked lane markings are compared with the ground truth. If their differences are smaller than a pre-defined threshold, a true positive detection is counted, otherwise a false negative. Because the system detects multiple lane markings, and the ground truth includes only the lane in which the vehicle is driving, it is clear that without the lane selection module this evaluation scheme can not generate the false positive statistic. The average lateral offsets difference and variance are calculated in pixel distance.

The evaluation database covers various challenging road situations. In figure 3 several typical images from video sequences are shown together with the tracking results. The videos are not only recorded on highways, but also on country roads and suburb areas. The shapes of the lanes are not only straight, sharp curves are also included, which are quite often at the entries or exits of the highways or on the country roads. There are also videos under adverse weather. The quality of the lane markings in the database is not consistent, worn out markings are also included. The illumination factor is also considered for the selection of the video sequences, e.g. the back-lighting situation shown in figure 3b. The back-lighting can cause a overall low contrast in the images, because of the dynamic range limitation of the digital camera sensor. Another difficult situation is the light interference during the night with raining. The head beams or tail lights of other traffics can cause interferences in the camera image, as shown in figure 3e. Because of its strip-form wrong detections could generated by an Hough-like line detection algorithm.

The false negative (FN), true positive (TP) and false positive (FP) are calculated in the same way as in [21]. In each frame f the number of ground truth markings is T^f , and the FN^f and TP^f are counted, N is the total number of frames. The average false negatives and true positives are

calculated as:

$$\overline{FN} = \frac{1}{N} \sum_{f=1}^N \frac{FN^f}{\max(T^f, 1)} \quad (15)$$

$$\overline{TP} = \frac{1}{N} \sum_{f=1}^N \frac{TP^f}{\max(T^f, 1)} \quad (16)$$

$$\overline{FP} = \frac{1}{N} \sum_{f=1}^N \frac{FP^f}{\max(T^f, 1)} \quad (17)$$

According to these definitions the FN, TP and FP are calculated in each frame separately, and the final results are the average values of all frames. The evaluation video set contains 49 videos with 14939 frames. The final statistics are shown in table I.

TABLE I: Final evaluation results

\overline{FN}	0.0249
\overline{TP}	0.9751
\overline{FP}	0.0116
Mean of the Lane Position Error	3.66px
Standard Deviation of the Lane Position Error	4.60px

V. CONCLUSION

The spline-based lane model has been introduced in lane marking detection and tracking area in [13], but its potentials and advantages against other models have never been fully explored. To our best knowledge the spline-based lane marking model has also for the first time been integrated into the extended Kalman filter in our method. We have demonstrated the simplicity, flexibility and robustness of this model using real and challenging video sequences, which are chosen to cover different problematic driving situations for a lane detection and tracking system.

The features of our system, like multiple lane tracking, ability to describe arbitrary form of lane markings, independent tracking of each lane marking, etc. provide the potential and possibility that it could be applied for various driving assistant applications.

ACKNOWLEDGMENT

This work was also supported by the European Commission under interactIVe, a large scale integrated project part of the FP7-ICT for Safety and Energy Efficiency in Mobility. The authors would like to thank all partners within interactIVe for their cooperation and valuable contribution.

REFERENCES

- [1] A. Borkar, M. Hayes, M. T. Smith, and S. Pankanti, "A layered approach to robust lane detection at night," in *Computational Intelligence in Vehicle and Vehicular Systems*, 2009.
- [2] J. C. McCall and M. M. Trivedi, "Video-based lane estimation and tracking for driver assistance: Survey, system, and evaluation," *IEEE Transactions on Intelligent Transportation Systems*, vol. 7, no. 1, pp. 20–37, March 2006.
- [3] C. Lipski, B. Scholz, K. Berger, C. Linz, T. Stich, and M. Magnor, "A fast and robust approach to lane marking detection and lane tracking," in *Proceedings of the 2008 IEEE Southwest Symposium on Image Analysis and Interpretation*, 2008.



Fig. 3: Examples from the evaluation database. The left side of a lane marking is highlighted with red line and the right side with cyan line.

- [4] S. Lee and W. Kwon, "Robust lane keeping from novel sensor fusion," in *Proceedings of the 2001 IEEE International Conference on Robotics and Automation*, 2001.
- [5] M. Meuter, S. Müller-Schneiders, A. Mika, S. Hold, C. Nunn, and A. Kummert, "A novel approach to lane detection and tracking," in *12th International IEEE Conference on Intelligent Transportation Systems*, 2009, pp. 1–6.
- [6] W. Liu, H. Zhang, B. Duan, H. Yuan, and H. Zhao, "Vision-based real-time lane marking detection and tracking," in *Proceedings of the 11th International IEEE Conference on Intelligent Transportation Systems*, 2008.
- [7] Q. Li, N. Zheng, and H. Cheng, "Springrobot: A prototype autonomous vehicle and its algorithms for lane detection," *IEEE Transactions on Intelligent Transportation Systems*, vol. 5, pp. 300–308, 2004.
- [8] S. Zhou, Y. Jiang, J. Xi, J. Gong, G. Xiong, and H. Chen, "A novel lane detection based on geometrical model and gabor filter," in *IEEE Intelligent Vehicles Symposium*, 2010.
- [9] M. Nieto, L. Salgado, F. Jaureguizar, and J. Arrospe, "Robust multiple lane road modeling based on perspective analysis," in *15th IEEE International Conference on Image Processing*, 2008, pp. 2396–2399.
- [10] *Richtlinien fuer die Markierung von Strassen RMS*, Forschungsgesellschaft fuer das Strassenwesen Std., 1980.
- [11] S. Nedevski, R. Schmidt, T. Graf, R. Danescu, D. Frentiu, T. Marita, F. Oniga, and C. Pocol, "3d lane detection system based on stereo-vision," in *2004 IEEE Intelligent Transportation Systems Conferences*, 2004.
- [12] B. Southall and C. Taylor, "Stochastic road shape estimation," in *Proceedings Eighth IEEE International Conference on Computer Vision*, 2001.
- [13] Y. Wang, D. Shen, and E. K. Teoh, "Lane detection using catmull-rom spline," in *1998 IEEE International Conference on Intelligent Vehicles*, 1998, pp. 51–57.
- [14] Y. Wang, E. K. Teoh, and D. Shen, "Lane detection and tracking using b-snake," *Image and Vision Computing*, vol. 22, pp. 269–280, 2004.
- [15] Z. Kim, "Robust lane detection and tracking in challenging scenarios," *IEEE Transactions on Intelligent Transportation Systems*, vol. 9, pp. 16–26, 2008.
- [16] A. Eidehall, F. and Gustafsson, "Combined road prediction and target tracking in collision avoidance," in *2004 IEEE Intelligent Vehicles Symposium*, 14 - 17 June 2004, pp. 619–624.
- [17] D. D. Hearn and M. P. Baker, *Computer Graphics with OpenGL*. Prentice Hall, 2004.
- [18] V. Lepetit and P. Fua, "Monocular model-based 3d tracking of rigid objects: A survey," *Foundations and Trends in Computer Graphics and Vision*, vol. 1, pp. 1–89, 2005.
- [19] Y. Bar-Shalom and X.-R. Li, *Multitarget-Multisensor Tracking: Principles and Techniques*. Y. Bar-Shalom, Ed. Yaakov Bar-Shalom, 1995.
- [20] A. Jain, M.N.Murty, and P.J.Flynn, "Data clustering: A review," *ACM Computing Surveys*, vol. 31, pp. 264–323, 1999.
- [21] K. Smith, D. Gatica-Perez, J. Odobez, and S. Ba, "Evaluating multi-object tracking," in *Proceedings of the 2005 IEEE Computer Society Conference on Computer Vision and Pattern Recognition*, 2005.